

See discussions, stats, and author profiles for this publication at: <https://www.researchgate.net/publication/229917222>

Electrooptical Properties of Liquid-Crystalline Rigid Rod-Like Polymers with NLO-Active Sidegroups

ARTICLE *in* BERICHTE DER BUNSENGESELLSCHAFT/PHYSICAL CHEMISTRY CHEMICAL PHYSICS · OCTOBER 1993

DOI: 10.1002/bbpc.19930971017

CITATIONS

4

READS

13

6 AUTHORS, INCLUDING:



Ladislav Kalvoda

Czech Technical University in Prague

48 PUBLICATIONS 220 CITATIONS

SEE PROFILE



Margit Schulze

Hochschule Bonn-Rhein-Sieg

55 PUBLICATIONS 622 CITATIONS

SEE PROFILE



Dieter Neher

Universität Potsdam

292 PUBLICATIONS 10,062 CITATIONS

SEE PROFILE

Electrooptical Properties of Liquid-Crystalline Rigid Rod-Like Polymers with NLO-Active Sidegroups

H.-J. Winkelhahn, Th. K. Servay, L. Kalvoda*), M. Schulze, D. Neher, and G. Wegner

Max-Planck-Institut für Polymerforschung, Ackermannweg 10, D-55128 Mainz, Germany

Key Words: Dielectrics / Liquid Crystals / Materials Properties / Nonlinear Phenomena / Polymers

The second order nonlinear susceptibility $\chi^{(2)}$ of a novel class of poled polymer films was investigated by means of the attenuated total reflection (ATR) method. The polymers are composed of an aromatic polyester backbone to which NLO active stilbene chromophores and flexible alkyl side chains are alternately attached. The optical properties and the dynamics of relaxation of the poled state were strongly depending on the length of the aliphatic side chains. The relaxation determined at different temperatures above and below T_g showed a temperature dependence that differs from an Arrhenius type behaviour. An empirical equation which relates the temperature dependence of the relaxation times to the glass transition temperature is presented.

The polyester main chains could be macroscopically aligned in strong magnetic fields. Electric poling of the samples with aligned main chains results in ratios of $\chi_{333}^{(2)}/\chi_{113}^{(2)}$ which deviate significantly from the ratio of 3 one obtains for samples with isotropically distributed main chains. This behaviour is explained by the solid state structure of this kind of polymer, which is best described by a sequence of alternating layers of polyester backbones and flexible side chains.

1. Introduction

The attractive mechanical and electronic properties of polymers make them excellent candidates for electrooptical applications such as in communication and information processing devices [1, 2]. To this end a number of different polymer systems have been developed [3]. Within the dipolar approach it is essential to have a macroscopically noncentrosymmetric distribution of dipoles with microscopical hyperpolarisabilities β (NLO chromophores) to obtain a linear electrooptical response (Pockels effect) from a material. While many NLO chromophores with sufficiently high β values have been developed, the lack of intrinsic interaction which would stabilize the noncentrosymmetric dipole distribution is the main problem for application of amorphous systems in Pockels devices. Organic crystals and Langmuir-Blodgett films can show an intrinsic noncentrosymmetric distribution of dipoles, whereas in spin-coated polymer films, which are the most promising candidates for waveguiding devices [2], there is no intrinsic interaction that aligns the dipoles. In this case the equilibrium dipole distribution is centrosymmetric. Due to the softening of amorphous systems above their glass transition temperature, one can pole these materials. During the poling procedure the NLO dipoles are aligned by a strong electric field at elevated temperatures, and the noncentrosymmetric dipole distribution is frozen in by cooling with the poling field still applied. After switching off the poling field, the materials relax to a centrosymmetric distribution again within a certain relaxation time. Fully aromatic polyesters decorated with alkoxy side chains are known to form layered structures in the solid state [4, 5]. Consequently, we developed the idea to replace some of the flexible alkoxy side chains by NLO chromophores and to investigate the influence of the intrinsic interaction leading to the formation of layers

on the relaxation properties of the poled state. The ATR method [6] has been shown to be a powerful tool to investigate the electrooptical properties of poled polymer films [7, 8, 9]. In particular, the ATR method is sensitive to optical anisotropies, offering the possibility to determine different components of the third rank nonlinear susceptibility tensor $\chi_{ijk}^{(2)}$.

2. Experimental

The polymers under investigation are shown in Fig. 1. The synthesis is described elsewhere [10, 11]. Two different derivatives have been investigated in detail with respect to their linear and nonlinear optical properties. Following the notation in [11] these are designated as C and D (C: $n = 2$, $m = 5$, $x = y$; D: $n = 5$, $m = 7$, $x = y$). The properties of a polyester with long alkyl side chains (B: $m = 2$, $n = 15$, $x = y$) are described in [11]. The DSC traces (Mettler DSC 30, heating rate of 10 K/min) of polymers C and D are shown in Fig. 2 and Fig. 3, respectively. One obtains glass transition temperatures $T_g(C) = 41^\circ\text{C}$, $T_g(D) = 48^\circ\text{C}$ and

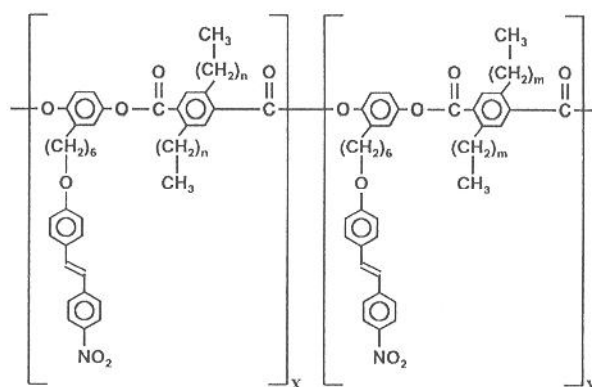


Fig. 1
Structure of Polymers

*) Permanent address: Inst. of Macromol. Chemistry, Heyrovsky Sq. 2, 16206 Prague 6, Czech Republic

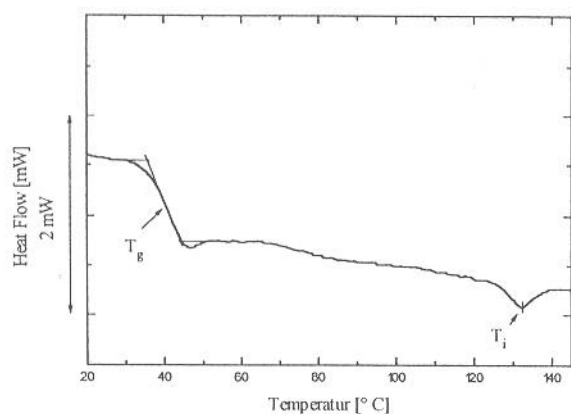


Fig. 2
DSC-Thermogram of Polymer C (second heating)

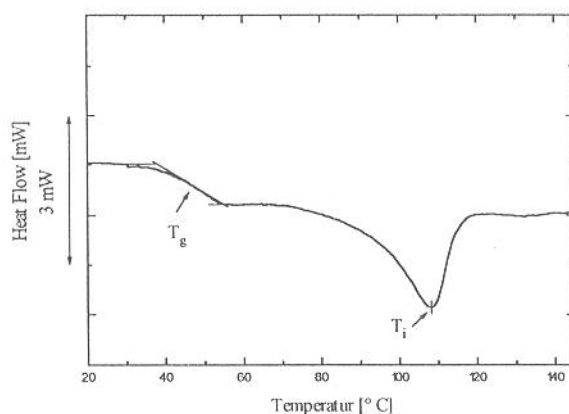


Fig. 3
DSC-Thermogram of Polymer D (second heating)

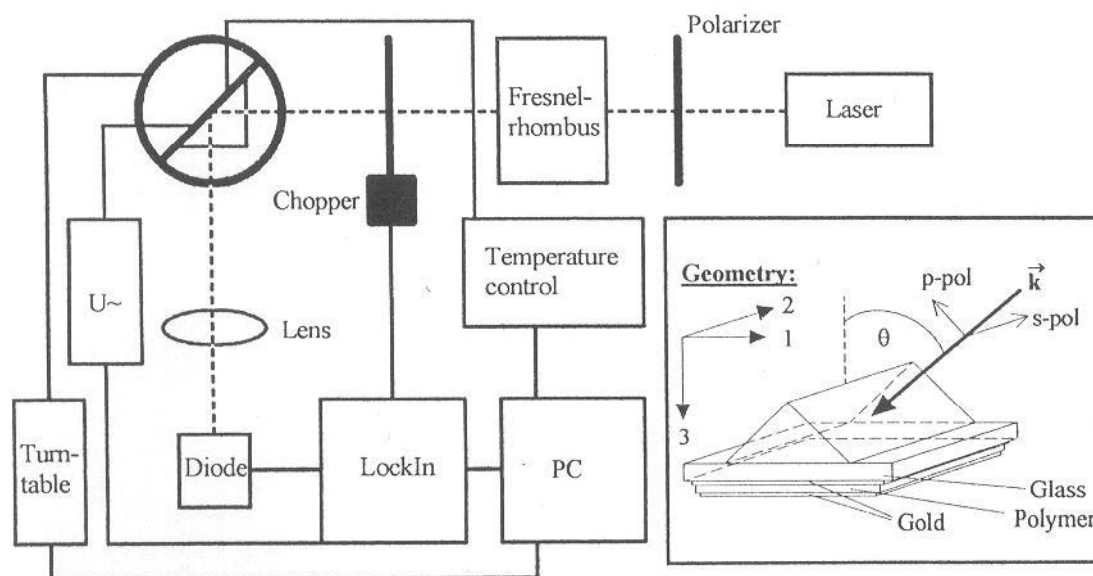


Fig. 4
Experimental setup of the ATR experiment

transitions to the isotropic state at $T_i(\text{C}) = 138^\circ\text{C}$, $T_i(\text{D}) = 110^\circ\text{C}$.

Samples for ATR experiments were prepared by spin coating a polymer-tetrachlorethane solution onto a 40 nm thick gold layer covering a BK7 glass substrate. Spinning conditions were chosen to obtain a film thickness of about 2 μm . After drying the films for 12 to 24 hours in a vacuum oven, a 100 nm gold film top electrode was evaporated onto the polymer. Magnetic field-aligned samples of polymer C were prepared by heating the polymer film above T_i in a 7 Tesla NMR magnet followed by a slow decrease in temperature down to room temperature over 7 to 10 hours. Electrode poling was performed for both polymers at $T_{\text{pol}} = 80^\circ\text{C}$ with poling fields of $E_{\text{pol}} = 40 \text{ V}/\mu\text{m}$. A cooling rate of $0.1^\circ\text{C}/\text{min}$ was used from T_{pol} to room temperature. In order to investigate the temperature dependence of the relaxation times the sample was heated up to different temperatures with a heating rate of $6^\circ\text{C}/\text{min}$. Then the poling field was switched off and the decay of the electrooptical signal was recorded.

The ATR setup with the geometric specifications is shown schematically in Fig. 4. In an ATR experiment the reflectivity of a multilayer system is measured for different incidence angles θ . The angular dependent spectra show significant dips which correspond to a coupling of the incident wave with one of the guided modes in the polymer film [7]. These modes are identical to the Fabry-Perot resonances of the layered system. The reflectivity spectra can be fitted to the Fresnel equations for multilayer systems with the film's refractive index and thickness as the fitting parameters. In Fig. 5 and Fig. 6 the reflectivity spectra of a film spin coated from polymer D are shown. Fig. 5 shows the TE-modes, which correspond to the light with the E -field parallel to the 2-direction in the sample. In Fig. 6 the TM-modes are shown. In this case the E -field has components parallel to the 1- and to the 3-directions. Assuming the spincoated film is isotropic in the 1–2-plane, the fitting procedure was accomplished as follows. First the TE-modes were fitted to fix the $\epsilon_{11} = \epsilon_{22}$ components of the dielectric tensor and the film thickness. After that the TM-modes were used to fit

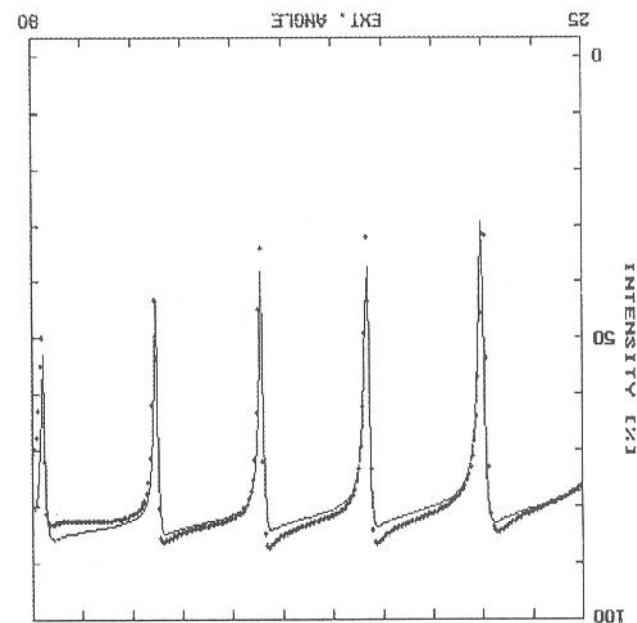


Fig. 5
Comparison between experimental (dots) TM-Modes of a 2.73 μm thick film of Polymer D and least square fit (solid line)

the ϵ_{33} value. As shown in Fig. 5 and 6 there is very good agreement between experiment and theory.
In order to obtain a good fit it was sometimes necessary to increase the imaginary part of the dielectric constants. A perfect film would yield a damping which corresponds to the absorption of the polymer at the measuring wavelength, in our case 633 nm. However, all film inhomogeneities such as surface roughness and scattering centers lead to an increase of the extrinsic damping.

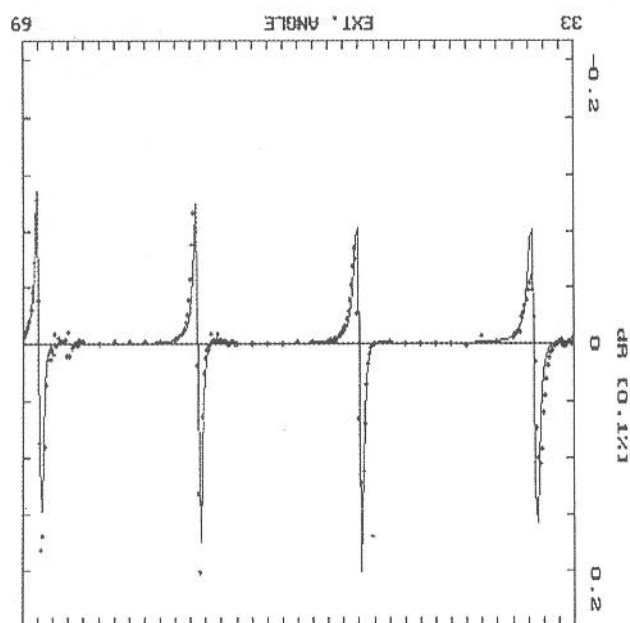


Fig. 7
Comparison between experimental (dots) and least square fit (solid line) values for the modulation of TF-Modes shown in Fig. 5

After polling along the 3-direction, the periodic change in reflectivity with an applied modulated field $E_m = E \cos(\omega t)$ is recorded as a function of the angular position. This change is directly related to the field dependent dielectric constant $\epsilon(E_m)$:

$$\epsilon_{ij}(E_m) = \epsilon_{ij}(0) + 2\chi_{ij3}^{(2)}E_m + \dots$$

and thickness $h(E_m)$:

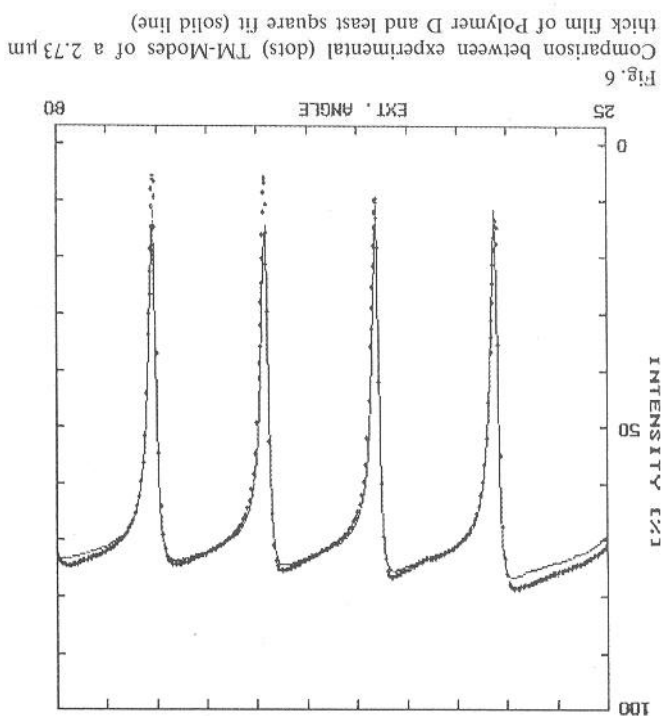


Fig. 6
Comparison between experimental (dots) TM-Modes of a 2.73 μm thick film of Polymer D and least square fit (solid line)

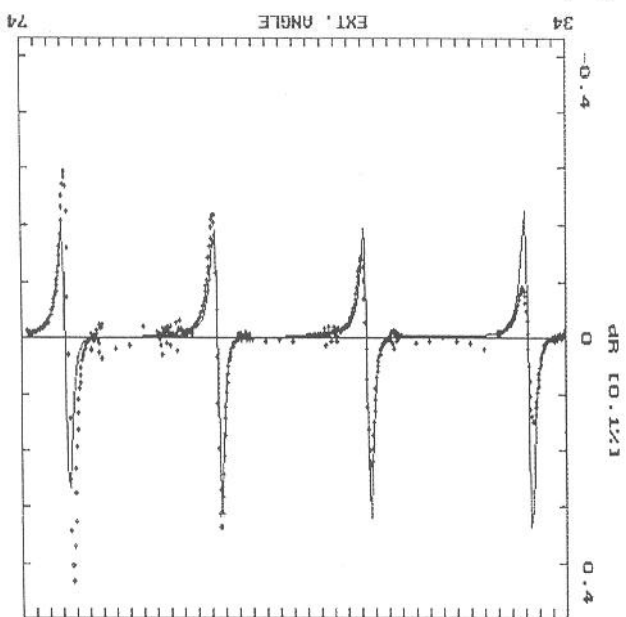


Fig. 8
Comparison between experimental (dots) and least square fit (solid line) values for the modulation of TM-Modes shown in Fig. 6

$$h(E_m) = h(0)(1 + dE_m + \dots)$$

In the above equation d is the piezoelectric constant of the poled film. The comparison between experiment and fit is shown in Fig. 7 for the TE-modes and in Fig. 8 for the TM-modes. Again, first the modulation spectrum for the s-polarized light is fitted yielding in values for $\chi_{223}^{(2)}$ and d . After this the scan with p-polarized light is fitted to obtain $\chi_{333}^{(2)}$.

3. Results and Discussion

3.1 Poling

In Table 1 the linear and nonlinear parameters are listed for a film of polymer D.

The ratio between the tensor components of $\chi^{(2)}$ is exactly 3 as expected for an isotropic film. Films of polymer C were poled with the same conditions as those of polymer D. The value $\chi_{333}^{(2)} = 11.8$ pm/V for this polymer is three times larger than the value obtained for polymer D. The ratio between the $\chi^{(2)}$ components is again three. Since the chromophore densities are almost the same in both polymers one would expect similar $\chi^{(2)}$ values for both polymers. Moreover the polymer B with $n = 2$, $m = 15$, $x = y$ showed negligible $\chi^{(2)}$ values after poling. This indicates a structural interaction – strongly depending on the side chain length – that hinders the poling process [12]. In fact, a pairing of the chromophore dipoles in the side chain layers for long side chains has been proposed [11]. The influence of the layered structure on the poling behaviour was investigated using samples of polymer C whose main chains were aligned in a strong magnetic field [13]. We prepared samples with main chains aligned either parallel to the 1- or

the 3-direction in the sample coordinate system. The order parameter was determined by X-ray diffraction to be $\langle P_2 \rangle = 0.85$ [11]. In the first case the electric poling field acts perpendicular to the previously applied magnetic field while in the second case both fields are parallel. In addition the chromophores are aligned by the magnetic field. However the absolute $\chi^{(2)}$ values are not influenced by this alignment for two reasons. First, the axial vector of the aligning magnetic field induces a centrosymmetric distribution, which produces no $\chi^{(2)}$ effect, and second the electric field poling is performed above the glass transition temperature of the material, where a strong increase in the side chain mobility occurs and all previously induced order among the side chains vanishes. The correlation of the glass transition temperature with the side chain mobility is based on NMR measurements for samples whose main chains have been partially deuterated [11].

If the main chains are aligned along the 3-direction, the symmetry of the samples, which determines the nonzero components of the $\chi^{(2)}$ tensor after poling, is still $C_{\infty v}$ as for unoriented samples. Orienting the main chains parallel to the 1-direction leads to C_{2v} symmetry. In this case, two measurements with different orientations between the light propagation direction k and the B -field vector are necessary to determine all components of $\chi^{(2)}$. We assume the sample coordinate system to coincide with the main axis system of the orientational symmetry. Therefore the experiment with k parallel to the 1-direction and s polarized light yields the 11 tensor components while a scan with p polarized light contains both the 22 and 33 tensor components of ϵ_{ij} and $\chi_{ij3}^{(2)}$ respectively. After rotating the sample 90° with respect to k , the s polarized measurement determines the 22 component, while p polarization gives the superposition of 11 and 33 components. Table 2 and Table 3 list the values for the

Table 1
Linear and nonlinear optical parameters obtained from the fits shown in Figs. 5, 6, 7 and 8

linear	$\epsilon'_{11} = \epsilon'_{22}$	$\epsilon''_{11} = \epsilon''_{22}$	ϵ'_{33}	ϵ''_{33}	h [μm]
	2.75	0.001	2.74	0	2.73
nonlinear	$\chi_{113}^{(2)} = \chi_{223}^{(2)}$ [pm/V]	$\chi_{113}^{(2)'} = \chi_{223}^{(2)'}$ [pm/V]	$\chi_{333}^{(2)}$ [pm/V]	$\chi_{333}^{(2)'}$ [pm/V]	d [pm/V]
	1.1	0.001	3.3	0.001	0

Table 2
Linear and nonlinear optical parameters obtained for a sample of Polymer C with main chains oriented parallel to the 1-direction

linear	pol.	ϵ'_{11}	ϵ''_{11}	ϵ'_{22}	ϵ''_{22}	ϵ'_{33}	ϵ''_{33}	h [μm]
$k \parallel B$	s	—	—	2.546	0.017	—	—	1.63
$k \parallel B$	p	2.762	0.031	—	—	2.55	0.031	1.63
$k \perp B$	s	2.762	0.031	—	—	—	—	1.63
$k \perp B$	p	—	—	2.546	0.017	2.55	0.031	1.63
nonlinear	pol	$\chi_{113}^{(2)}$ [pm/V]	$\chi_{113}^{(2)'}$ [pm/V]	$\chi_{223}^{(2)}$ [pm/V]	$\chi_{223}^{(2)'}$ [pm/V]	$\chi_{333}^{(2)}$ [pm/V]	$\chi_{333}^{(2)'}$ [pm/V]	d [pm/V]
$k \parallel B$	s	—	—	7.25	0.5	—	—	−3.92
$k \parallel B$	p	7.85	0.45	—	—	14.75	−1.9	−3.92
$k \perp B$	s	7.85	0.45	—	—	—	—	−3.92
$k \perp B$	p	—	—	7.25	0.5	9.45	−0.45	−3.92

Table 3

Linear and nonlinear optical parameters obtained for a sample of Polymer C with main chains oriented parallel to the 3-direction

linear	$\epsilon'_{11} = \epsilon'_{22}$	$\epsilon''_{11} = \epsilon''_{22}$	ϵ'_{33}	ϵ''_{33}	$h [\mu\text{m}]$
	2.9	0.044	2.89	0.04	2.0
nonlinear	$\chi_{113}^{(2)} = \chi_{223}^{(2)} [\text{pm/V}]$	$\chi_{113}^{(2)''} = \chi_{223}^{(2)''}$	$\chi_{333}^{(2)} [\text{pm/V}]$	$\chi_{333}^{(2)''} [\text{pm/V}]$	$d [\text{pm/V}]$
	2.91	0.06	10.77	1.76	-0.044

linear and nonlinear parameters obtained for a main chain orientation parallel to the 1- and 3-direction respectively.

The anisotropy which was induced in the samples by aligning the main chains in a strong magnetic field significantly affects the ratios of the $\chi^{(2)}$ components. Aligning the main chains parallel to the direction of electric poling field yields a ratio $\chi_{333}^{(2)}/\chi_{113}^{(2)} = 3.7$, while in the case of a perpendicular orientation between electric poling field and preferred main chain direction, a ratio of $\chi_{333}^{(2)}/\chi_{113}^{(2)} = 1.6$ is obtained. This is in agreement with the proposed molecular orientation of a sample shown schematically in Fig. 9. In this picture, the sample consists of an alternating stack of side and main chain layers. During the poling process the chromophores can easily move inside the side chain layers while the movement through the main chain layers is strongly hindered. The magnetic alignment of the main chains induces a preferred orientation of the main chain layers. A magnetic field parallel to the 3-direction produces an isotropic orientation distribution in the 1,2-plane of the vectors normal to the main chain layers, while in the case of aligning the main chains along the 1-direction, these normal vectors are isotropically distributed in the 2,3-plane. Consequently an electric poling parallel to the 3-direction yields different $\chi_{333}^{(2)}/\chi_{113}^{(2)}$ ratios, taking into account the structural interaction between chromophores and main chain layers.

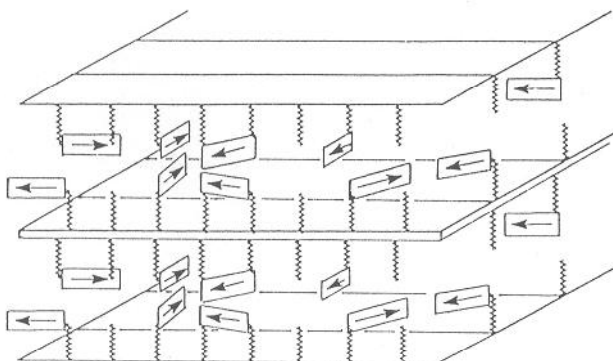


Fig. 9
Schematic representation of molecular order

3.2 Relaxation

In order to determine the relaxation times for the induced noncentrosymmetric chromophore distribution, the angular position was fixed to the waveguide mode with the highest

nonlinear modulation and the decay of the modulation signal was measured for certain times. Since the maximum value for a modulated waveguide mode is proportional to the actual $\chi^{(2)}$ value, the decay in modulation amplitude is a measure of the decrease in polar order. The relaxation times at a temperature of 25 °C for two different cooling rates of 1 °C/min and 0.1 °C/min are compared in Fig. 10. In both cases the time dependence of relaxation was best fitted with a Kohlrausch-Williams-Watts (KWW) function as observed by other groups [15, 16]:

$$\frac{\Delta R(t)}{\Delta R(0)} = \exp[-(t/\tau_{\text{KWW}})^\beta] = \frac{\chi^{(2)}(t)}{\chi^{(2)}(0)}$$

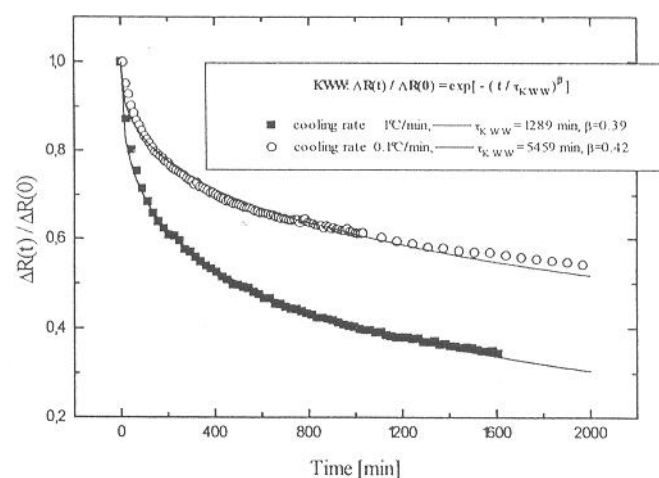


Fig. 10
Relaxation time dependence on cooling rate at 298 K for Polymer C

A lower cooling rate strongly increases the relaxation time. This can be understood in terms of the free volume the chromophores require to change their orientation. Since the free volume relaxes to the equilibrium distribution faster at higher temperatures, annealing just below T_g [14] or cooling down with a slow rate should result in a smaller free volume fraction remaining. All subsequent relaxation data were obtained with a cooling rate of 0.1 °C/min. The relaxation behaviours of the polymers C and D are compared in Fig. 11 for two relaxation temperatures, 25 °C and 50 °C. There is a large difference in the temperature dependence of the relaxation times due to higher glass transition temperature of polymer D. In contrast to NLO polymers based on

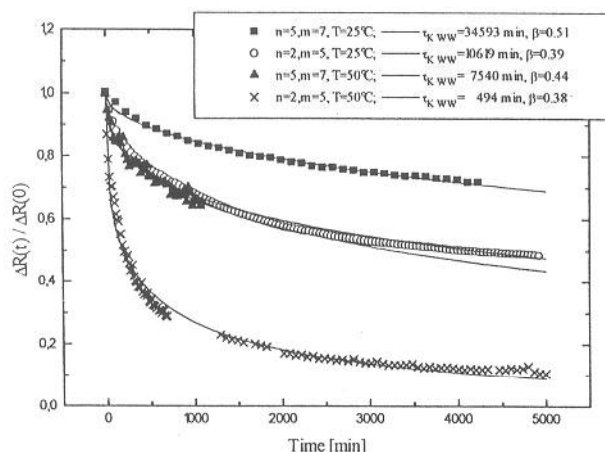


Fig. 11
Relaxation time dependence on side chain length

the guest-host concept or polymers with chromophores connected to flexible main chains, the polyesters investigated here show relaxation times in the range of hours even above their glass transition temperatures [19, 15]. Since the glass transition temperature is related to the side chain motion as mentioned above, this unusual relaxation behaviour also gives evidence for an interaction between the chromophores and the main chain layers. The small deviations between the experimental values and the fits with the KWW function are attributed to physical aging of the sample during the measurement. This aging behaviour is not included in the KWW function. A weighting factor can be introduced to the KWW function to yield

$$\frac{\Delta R(t)}{\Delta R(0)} = K \cdot t^{-\kappa} \cdot \exp[-(t/\tau_{\text{KWW}})^\beta]$$

which results in a better fit to the time dependence. Different samples of polymer C were poled to obtain the temperature dependence of the relaxation times. For each temperature the decay curves were fitted with both a biexponential function and with the KWW function. For higher temperatures the fitted τ_{KWW} approaches the value for the shorter time constant of the biexponential relaxation, while for lower temperatures a τ_{KWW} comparable to the longer time constant of the biexponential fit was found. A distribution of relaxation times is commonly found for relaxation experiments in the frequency domain [7]. Since the time domain KWW function is related to the widely used Havriliak-Negami function in the frequency domain [18], a distribution of relaxation times should be used to describe the poling relaxation. The temperature dependence of the poling relaxation is compared with relaxation times obtained from dielectric spectroscopy [10] in Fig. 12. The dielectric data are very well fitted by a WLF temperature dependence with parameters $C_1 = 12$, $C_2 = 59$, $T_g = 40^\circ\text{C}$. The temperature dependence for poling relaxation times follows a function which was empirically found to be:

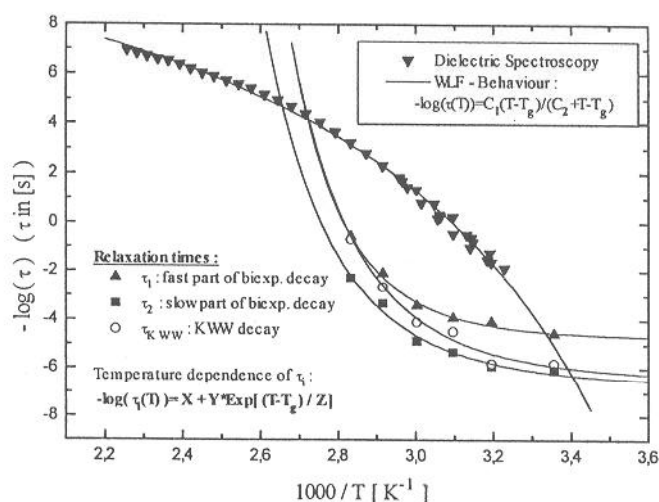


Fig. 12
Comparison between activation of the dielectric WLF-process and poling relaxation in Polymer C

$$-\log(\tau(T)) = X + Y \cdot \exp\left[\frac{T - T_g}{Z}\right]$$

The poling relaxation shows a significant deviation from the dielectric relaxation. However dielectric spectroscopy probes the relaxation of dipoles in thermal equilibrium, while the decay experiment measures the relaxation from a frozen-in perturbed state prepared at an elevated temperature with an electric field applied. There is a relation between the WLF function and the empirical equation which describes the temperature dependent poling relaxation. Computing the first derivative of $-\log(\tau_{\text{WLF}})$ versus temperature leads to a function whose inverse is integrated with temperature as variable. The resulting function gives a very good fit to the temperature dependent poling relaxation. On the other hand, one can repeat the mathematical treatment – differentiation versus temperature, computing the reciprocal and integrating with temperature as the variable – with the empirical equation to obtain an equation which fits the WLF behaviour. The reciprocity between these two functions leads to a relation between free volume and re-

laxation rate. Using the fractional free volume $f = \frac{v_f}{v_t} = f_g + \alpha(T - T_g)$ and the Doolittle equation $\eta \sim \exp[b/f]$ as the elements of the WLF function [17], the above procedure yields the following form for the orientational relaxation times:

$$-\log(\tau) \sim \int_{T_1}^T \frac{[f_g + \alpha(T - T_g)]^2}{b\alpha} dT$$

which shows a hyperexponential dependence of the relaxation times on free volume. Further investigations with different cooling rates will be necessary to confirm this dependence.

4. Conclusion

The nonlinear optical properties of polyesters substituted with NLO-active chromophores and flexible side chains of variable length have been investigated by the ATR method. For short side chains (Polymer C) we obtained an electrooptic coefficient $r_{33} = 1.5 \text{ pm/V}$ using a poling field of $40 \text{ V}/\mu\text{m}$. Increasing the length of aliphatic side chains strongly reduces the electrooptic coefficient but at the same time improves the longterm stability due to a higher glass transition temperature. The influence of the free volume on relaxation times was demonstrated by varying the cooling rates during the poling process. The time dependence of the relaxation process is best described by a KWW function. Aging effects can be described by adding a weighting factor to the KWW function. The temperature dependence of the relaxation times deviates from an Arrhenius-type and from a WLF behaviour. An empirical function related to the glass transition temperature and linked to the WLF function was found to describe the temperature dependence of relaxation times. Relaxation times in the range of hours are obtained even 20° above the glass transition. We were able to align the polyester main chains in a strong magnetic field. The resulting anisotropy affects the electric poling of chromophores. For unoriented samples, ratios of $\chi_{333}^{(2)}/\chi_{113}^{(2)}$ equal to three were found, but this ratio deviates strongly from three for oriented samples. Orienting the main chains parallel to the electric poling field increases the ratio to 3.7 while a perpendicular orientation between preferred main chain direction and electric poling field decreases the ratio to 1.6.

We thank Dr. F. Kremer and E. Aust for many helpful discussions. This work was financially supported by the German ministry of research and technology (BMFT) under project number 03M4046.

References

- [1] R. Lytel, G.F. Lipscomb, E.S. Binkly, J.T. Kenney, and A.J. Ticknor, ed. by S.R. Marder, J.E. Sohn, and G.D. Stucky, in ACS Symposium Series 455, 103, 1991.
- [2] George I. Stegeman, ed. by S.R. Marder, J.E. Sohn, and G.D. Stucky, ACS Symposium Series 455, 113, 1991.
- [3] D. Li, J. Yang, C. Ye, M.A. Ratner, G. Wong, and T.J. Marks, in "Nonlinear optical and electroactive polymers" ed. by P.N. Prasad and D.R. Ulrich, Plenum Press, p. 217, 1988.
- [4] M. Ballauf, *Angew. Chem.* 101, 261 (1989).
- [5] C. Schrauwen, T. Pakula, and G. Wegner, *Makromol. Chem.* 193, 11 (1992).
- [6] E. Kretschmann, *Z. Phys.* 241, 313 (1971).
- [7] M. Dumont, Y. Levy, and D. Morichere, *Organic Molecules for Nonlinear Optics and Photonics*, Kluwer Academic Publishers, p. 461, 1991.
- [8] S. Herminghaus, Barton A. Smith, and J.D. Swalen, *J. Opt. Soc. Am. B* 8 (11), 2311 (1991).
- [9] R.H. Page, M.C. Jurisch, B. Beck, A. Sen, R.J. Twieg, J.D. Swalen, G.C. Bjorklund, and C.G. Willson, *J. Opt. Soc. Am. B* 7, 1239 (1990).
- [10] Th. K. Servay, Dissertation, Universität Mainz (1993).
- [11] Th. K. Servay, H.-J. Winkelhahn, L. Kalvoda, M. Schulze, C. Boeffel, D. Neher, and G. Wegner, *Ber. Bunsenges. Phys. Chem.* (1993).
- [12] K.D. Singer, M.G. Kuzyk, T. Fang, W.R. Holland, and P.A. Cahill, *Organic Molecules for Nonlinear Optics and Photonics*, Kluwer Academic Publishers, p. 105, 1991.
- [13] S.I. Stupp, H.C. Lin, and D.R. Wake, *Chem. Mater.* 4, 947 (1992).
- [14] W. Köhler, D.R. Robello, P.T. Dao, C.S. Willand, and D.J. Williams, *Mol. Cryst. Liq. Cryst. Sci. Technol. - Sec. B: Nonlinear Opt.* 3, 83 (1992).
- [15] H.L. Hampsch, Jian Yang, G.K. Wong, and J.M. Torkelson, *Macromolecules* 23, 3640 (1990).
- [16] G.A. Lindsay, R.A. Henry, J.M. Hoover, A. Knoesen, and M.A. Mortazavi, *Macromolecules* 25, 4888 (1992).
- [17] N.G. McCrum, B.E. Read, and G. Williams, *Anelastic and dielectric effects in polymeric solids*, Dover Publications, Inc. 1967.
- [18] F. Alvarez, A. Alegria, and J. Colmenero, *Phys. Rev. B* 44 (14), 7306 (1991).
- [19] M. Eich, A. Sen, H. Looser, G.C. Bjorklund, J.D. Swalen, R. Twieg, and D.Y. Yoon, *J. Appl. Phys.* 66 (6), 2559 (1989).

Presented at the 92nd Annual Meeting of the Deutsche Bunsen-Gesellschaft für Physikalische Chemie "Neue Eigenschaften und Anwendungen von Flüssigkristallen" in Leipzig, from May 20th to May 22nd, 1993

E 8426